Temporal Correlation of the RSS Improves Accuracy of Fingerprinting Localization

Mei Wang*, Zhehui Zhang*, Xiaohua Tian*†, Xinbing Wang*†
*School of Electronic, Info. & Electrical Engineering, Shanghai Jiao Tong University, China
†National Mobile Communications Research Laboratory, Southeast University, China
{mary1994, qiaomai, xtian, xwang8}@sjtu.edu.cn

***Abstract*—Indoor localization based on RSS fingerprinting approach has been attracting many research efforts in the past decades. Recent study presents a fundamental limit of the approach: given requirement of estimation accuracy, reliability of the user's localization result can be derived. As highly accurate indoor localization is essential to enable many location based services, a natural question to ask is: can we further improve the accuracy of the localization scheme fundamentally? In this paper, we theoretically show that the temporal correlation of the RSS can improve accuracy of the RSS fingerprinting based indoor localization. In particular, we construct a theoretical framework to evaluate how the temporal correlation of the RSS can influence the reliability of location estimation, which is based on a newly proposed radio propagation model considering the time-varying property of signals from a given Wi-Fi AP. Such a theoretical framework is then applied to analyze localization in the one dimensional physical space, which reveals the fundamental reason why performance improvement of localization can be brought by temporal correlation of the RSS. We further extend our analysis to high-dimensional scenarios. Experimental results corroborate our theoretical analysis.**

I. Introduction

Indoor localization based on RSS fingerprinting approach has been attracting many research efforts in the past decades, where the basic idea is to first construct RSS fingerprints database during the training phase, and then perform location estimation by matching the user's reported fingerprints in the database during the localization phase [1]. Indoor localization systems based on the approach have been developed with different flavors. Embedded sensors of mobile devices are exploited to improve accuracy of the location estimation [2], [3], crowdsourcing paradigm is used to reduce the cost of site survey in the training phase [4], and machine learning algorithms are leveraged to shorten the delay of localization process [5]–[7].

The spring-up of RSS fingerprinting based indoor localization systems promotes efforts to study performance bounds of such systems both empirically and theoretically. Empirical studies evaluate performance of localization systems with comprehensive experiments. Liu *et al.* present their experimental results showing that the location estimation error could be over 6m [2]. Chandrasekaran *et al.* provide empirical quantification of accuracy limits of RSS localization, which is based on extensive experimental results conducted over a uniform testbed [8]. Such results could be helpful references for system implementation but hardly provide insight into the RSS fingerprinting approach. Some theoretical studies about localization performance bound are based on Cramér-Rao Bound (CRB) analysis [9]–[11]; however, that framework is based on the Log-Distance Path Loss (LDPL) radio propagation model [1], [8], which however has been proved inaccurate in the indoor localization scenarios [12].

Recently, Wen *et al.* present a theoretical investigation on RSS fingerprinting based indoor localization, which reveals fundamental limits of the localization methodology [13]. Specifically, the work derives a close-form expression for calculating the probability that a user can be correctly localized in a region of certain size, which is termed as localization reliability. The basic idea of the derivation is to build a probability space induced from RSS samples obtained from the training stage. The location determination process can be regarded as a mapping from the sample space to the physical space; therefore, the probability a user can be correctly localized in a certain region is equal to the probability that certain outcomes of RSS measurements appear, so that the localization system can determine the user's location to be in the region. As highly accurate indoor localization is essential to enable many location based services, a natural question to ask is: can we further improve the performance of the localization scheme fundamentally?

In this paper, we show that the temporal correlation of the RSS can improve accuracy of RSS fingerprinting based indoor localization. We first construct a theoretical framework to evaluate how the temporal correlation of the RSS can influence the reliability of location estimation, which is based on a newly proposed radio propagation model considering the time-varying property of signals from a given Wi-Fi AP. Based on such a model, we build a new sample space from the training phase, where each outcome in the space is extended with a new temporal dimension. With such a framework, the fingerprints used to estimate the users location are actually the correlation of the RSS observed from the AP.

We then apply such a theoretical framework to analyze localization in the one-dimensional physical space, which reveals the fundamental reason why performance improvement of localization can be brought by temporal correlation of the RSS. An interesting finding is that: the boundary in the sample space, which is used to distinguish one physical location from another, in fact should be one edge of hyperbola, instead of a straight line as believed in [13]; moreover, we

find that the curvature of the hyperbola is related to the correlation of the RSS in the sample space. Such a result can fundamentally improve accuracy of location estimation of the RSS fingerprinting based system.

We further extend our analysis to high-dimensional scenarios, where two-dimensional physical space and high temporal dimensions are taken into account. The major challenge incurred by the high dimension is the large number of variables, which hinders revealing the insight of the RSS fingerprinting approach. We derive a transformation matrix, which represents the linear affine transformations in Euclidean space like translation, rotation, and shearing, to deal with the challenge. We theoretically prove that the boundary in the sample space dividing two physical locations is a high-dimensional hyperbolic plane.

The remainder of the paper is organized as follows. Section II presents related work. Section III illustrates the service model. Section IV presents our analysis of localization with one-dimensional physical space, sample space and two-dimensional temporal space. Section V extends our analysis to higher dimensional cases. Section VI presents experimental results. The conclusion remarks and future work are provided in Section VII.

II. Related Work

A. Fundamental Limits of RSS Fingerprinting Approach

Wen *et al.* present a theoretical investigation on RSS fingerprinting based indoor localization, which reveals fundamental limits of the localization methodology [13]. Specifically, if a user's real location is at Q, the work derives a close-form expression of the probability R that the user can be localized in the δ neighborhood of Q, where δ and R are localization accuracy and reliability, respectively.

With the RSS fingerprinting based localization approach, RSS fingerprints obtained from the training stage form a sample space, based on which a user's location in the physical space can be estimated. The location determination process can be regarded as a mapping from the sample space to the physical space. If outcomes of RSS measurements fall into the event region $\mathbb{E}$, then the localization system can correctly determine the location of the user to be in the δ neighborhood of Q; therefore, the localization reliability is equal to the probability that outcomes of RSS measurements fall into the event region $\mathbb{E}$. By constructing a general radio propagation model based on field observations of real localization systems, probabilities for outcomes of RSS measurements in a location can be presented, which turns out to be following Gaussian distribution. Consequently, calculating the localization reliability is to first find the event region $\mathbb{E}$ in the RSS sample space, and then perform integration over the region $\mathbb{E}$ for an Gaussian probability density function (PDF).

Although utilizing a general radio propagation model, the study in [13] is distinguishable from the model based localization because the radio propagation model is not used to derive geometric relationships between signal transmitters and receivers, such as distance, time of arrival (ToA), time difference of arrival (TDoA) or angle of arrival (AoA) [1]. That is why the radio propagation model used in [13] only assumes that the mean of RSS readings varies with respect to locations but does not specify how the mean will vary. This is in contrast to the Log-Distance Path Lose (LDPL) model used in the model based localization and CRB analysis [9]–[11], where the mean varies with respect to locations logarithmically. Moreover, interesting findings about the shape of the event region $\mathbb{E}$ are presented in [13], where skillful mathematical techniques are demonstrated.

Our study constructs a new radio propagation model considering the temporal correlation of the RSS, which is not taken into account in [13]. The later discussions are to reveal that the boundary distinguishing one location from another in the sample space is different from that shown in [13], and the new boundary provides a more accurate location estimation. Compared with the pure theoretical analysis presented in [13], we present experimental results to validate our theoretical analysis.

B. Temporal Information of RSS Utilized for Localization

Kaemarungsi *et al.* study properties of the RSS for fingerprinting based localization using Wi-Fi [14]. Comprehensive experiment results reveal two important features of the RSS: First, the mean and variance of the RSS in one location basically remain the same over time; second, the auto-covariance function of the RSS in one location has the same shape for separate time-series. Based on such two observations, our work in this paper models the RSS observed in one location as a stationary process. Fang *et al.* propose a localization approach based on the dynamic system and machine learning technique [6]. Such an approach estimates the user's location by the state consisting of RSSes observed in different times and locations. However, the simple combination of spatial and temporal information does not reveal the essence how the temporal information can be utilized for localization, where the RSS observed in different times can be considered as multiple measurements of fingerprints.

Most of the current studies for utilizing temporal information of the RSS for localization are in a machine-learning based manner [5], [7], where the convincing explanation how the temporal information can influence the performance of the localization process is still unavailable. In this paper, we initiate the theoretical study on this issue.

III. Theoretical Model of Location Estimation

Consider an indoor space, which can be modeled as one or two dimensional Cartesian space denoted by $L \subset \mathbb{R}$ or $L \subset \mathbb{R}^2$, respectively. Examples of one dimensional model include hallway and corridor. A user's location in the physical space S can be denoted by $\mathbf{r} = r_1$ or $\mathbf{r} = (r_1, r_2)$ with corresponding dimensions. Based on the localization database constructed in the training phase, a sample space of fingerprints can be induced, which is denoted by Ω^n and n is the number of access points (APs) can be sensed in the physical space. In the training phase, the site surveyor collects fingerprints of

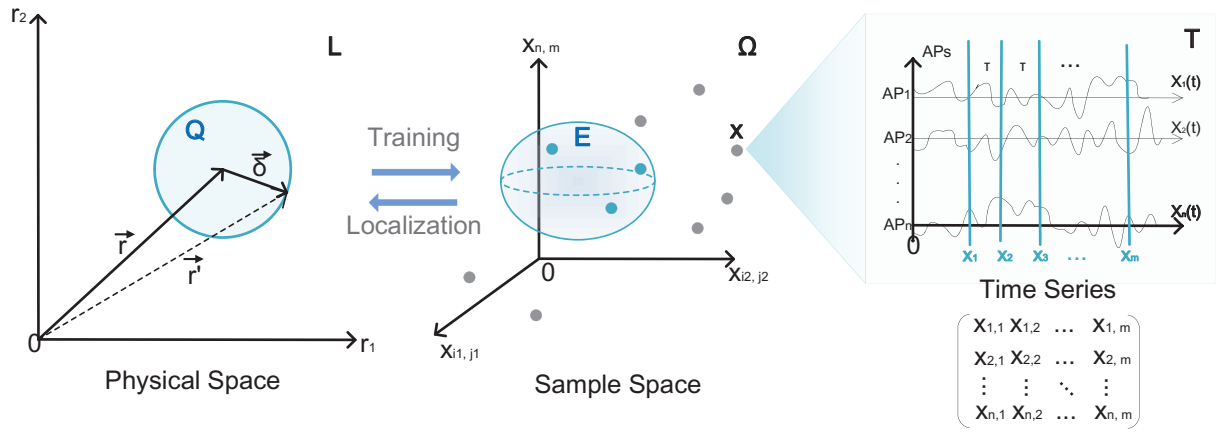

Fig. 1. Theoretical localization model.

APs in a one-by-one manner at a given location. For an AP, the surveyor samples the observed RSS at certain frequency. Consequently, if there are n APs and each AP is sampled m times, then a point $\mathbf{x}$ in the RSS sample space is in the following form:

$$\begin{bmatrix} x_{1,1} & x_{1,2} & \cdots & x_{1,m} \\ x_{2,1} & x_{2,2} & \cdots & x_{2,m} \\ \vdots & \vdots & \ddots & \vdots \\ x_{n,1} & x_{n,2} & \cdots & x_{n,m} \end{bmatrix}$$

where $x_{i,j}$ means the RSS observed with respect to AP_i at jth time point. We say this is an n-dimensional sample space and the temporal dimension of sampling is m.

As the radio propagation in the indoor environment is influenced by many factors such as path loss, shadowing, fading and multipath effect, the signal can be observed in a location is usually modeled as a random process, which can be denoted as

$$X(\mathbf{r}, \mathbf{t}) = S(\mathbf{r}) + \sigma Y(\mathbf{r}, \mathbf{t}), \tag{1}$$

where $\mathbf{r}$ is the location of the observation and $\mathbf{t}$ represents the vector of time points at which RSSes are observed. $S(\mathbf{r})$ is the trend model of the signal with respect to position $\mathbf{r}$ in the perspective of stochastic processes, and σ is the amplitude of noise. $Y(\mathbf{r}, \mathbf{t})$ is the joint Gaussian distribution of temporal noise series at location $\mathbf{r}$.

According to extensive experimental results and theoretical analysis [15]–[17], the mean and variance of the RSS in one location basically remain the same over time and the auto-covariance function of the RSS in one location has the same shape for separate time-series, such a random process can be stationary and ergodic, with

$$S(\mathbf{r}') \approx S(\mathbf{r}) + \bigtriangledown S(\mathbf{r})(\mathbf{r}' - \mathbf{r}) \tag{2}$$

In the localization phase, a user reports observed RSSes to the localization server, which then estimates the corresponding location by matching the reported fingerprints in the fingerprints database. Such a process can be modeled as a mapping from the sample space to the physical space:

$$M : \Omega^n \to L, \quad \mathbf{r}' = M(\mathbf{X}(\mathbf{r}, \mathbf{t})), \tag{3}$$

where $\mathbf{r}'$ is the estimated location of the user. This process is illustrated in Fig. 1. The user's actual location is at $\mathbf{r}$ and the estimated location is at $\mathbf{r}'$, which incurs the localization error denoted by $\vec{\delta}$.

Due to estimation errors, the result of the localization is that the user's location is estimated to be in the δ neighborhood of $\mathbf{r}$, which is denoted by Q. To reduce the error of localization is equivalent to mitigating the norm of $\vec{\delta}$. Since the basis of the estimation is the reported fingerprint by the user, the ideal case is that the user's submitted fingerprints happen to make the system believe that the location of the user is in Q. We use $\mathbb{E}$ to denote such a region in the sample space, so that the user's location can be estimated to be in Q as long as the reported RSSes fall in $\mathbb{E}$.

The probability that the reported RSS fingerprints can fall into the region of $\mathbb{E}$ depends on the model of radio signal propagation, which in fact fundamentally determines the performance of the RSS fingerprinting based approach. The model proposed in [13] considers the observed RSS at one location as a random variable, where temporal correlation of the signal is not taken into account. According to the site survey practice, it is more practical to model the signal as a random process as in this paper, where the temporal correlation can be leveraged. Our investigation in the rest of the paper is to show that such a seemingly slight change in the radio signal propagation modeling brings about not only much higher difficulties in mathematical analysis, but also interesting findings of the RSS fingerprinting based approach, which have never been revealed.

IV. Analysis of 2-D Temporal Correlation for 1-D Localization

This section examines a concrete scenario of localization, where both the physical space and the sample space are one

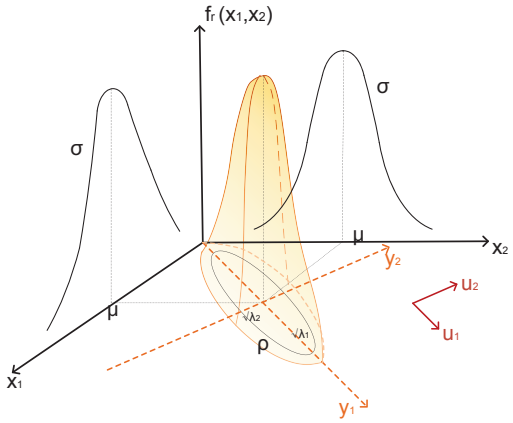

Fig. 2. Joint Gaussian PDF of $RSS(t)$ and $RSS(t+\tau)$ at position $\mathbf{r}$

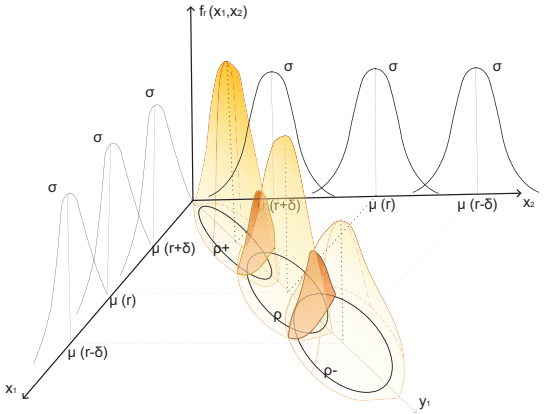

Fig. 3. Joint Gaussian PDFs at Different Locations.

dimensional and the temporal dimension of sampling is two. The purpose of the examination is to find how likely the user can be localized in Q with given δ. It is easier to reveal essence of the fingerprinting approach by analyzing a simple case, where the results could be inspiring for analyzing more complicated scenarios.

A. Finding Region $\mathbb{E}$

Let us first find out what kind of RSSes can be observed at the location $\mathbf{r}$. The one-dimensional physical space can be regarded as an one-dimensional horizontal axis, where the origin of the axis is the location of the AP, and the location of each point can be identified by a scalar r. Based on our proposed radio signal propagation model, the probability density function (PDF) of RSS readings can be observed follows the Multivariate Guassian Distribution, which is denoted by

$$f_r(x_1, x_2) = \frac{1}{2\pi\sigma^2\sqrt{1-\rho^2}} e^{-\frac{1}{2}\Delta^2}, \tag{4}$$

where x_1, x_2 are variables representing the RSSes at time points t_1 and t_2 separated by a duration of τ. Figure 2 illustrates $f_r(x_1, x_2)$. Since the random process representing the signal is stationary, the following analysis is oblivious to the specific value of t_1 and t_1 as long as they are separated by τ. Symbols μ and σ are the mean and standard variance of the RSS joint distribution at position $\mathbf{r}$, respectively; ρ is the autocorrelation coefficient of $f_r(x_1, x_2)$. The Mahalanobis distance is denoted as Δ, where

$$\Delta^2 = \frac{1}{\sigma^2(1-\rho^2)}[(x_1-\mu)^2+(x_2-\mu)^2-2\rho(x_1-\mu)(x_2-\mu)]. \tag{5}$$

Since x_1 and x_2 are both observed at r, the corresponding marginal distributions with respect to x_1 and x_2 are the same, according to our signal propagation model, and the corresponding means and standard variances of the two marginal distributions are the same as well. This also complies with the conclusion in [13]. Consequently, the covariance matrix of $f_r(x_1, x_2)$ is real, positive and symmetric, where

$$\mathbf{\Sigma} = \sigma^2 \begin{bmatrix} 1 & \rho \\ \rho & 1 \end{bmatrix}. \tag{6}$$

With the same reason, the major axis of the elliptical surface representing $f_r(x_1, x_2)$ should be the angular bisector of the Cartesian coordinates with slope 1.

In order to facilitate our analysis, we put the image of $f_r(x_1, x_2)$ in a new coordinates system with axes y_1 and y_2. We let the major axis of the elliptical surface align to y_1 and the origin of the new coordinates system be $(\mu(r), \mu(r))$ in the old system. Then the PDF in the new system is

$$f_r(y_1, y_2) = \frac{1}{2\pi\sigma^2\sqrt{\lambda_1\lambda_2}} e^{-\frac{1}{2\sigma^2}(\frac{y_1^2}{\lambda_1}+\frac{y_2^2}{\lambda_2})}, \tag{7}$$

where

$$\lambda_1 = \frac{\sqrt{2}(1+\rho)}{2}, \lambda_2 = \frac{\sqrt{2}(1-\rho)}{2}. \tag{8}$$

We now start to find the region $\mathbb{E}$ in this scenario. Refer to Fig. 3, the value of $f_r(y_1, y_2)$ in fact means how likely the user can observe $[y_1, y_2]$ at location r. If the reported RSSes $[y_1, y_2]$ indicate that the user's location is in a small neighborhood of r, then $f_r(y_1, y_2)$ should be higher than $f_{r\pm\delta}(y_1, y_2)$, where $r\pm\delta$ are boundaries of r's neighborhood in the physical space. That is, if the user is localized in the neighborhood of r, the corresponding submitted fingerprints should have fallen into the region

$$\mathbb{E} = \{\mathbf{x} | f_r(\mathbf{y}|\mu(r), \mathbf{\Sigma}(r)) \geq f_{r\pm\delta}(\mathbf{y}|\mu(r\pm\delta), \mathbf{\Sigma}(r\pm\delta))\}. \tag{9}$$

The profile of $\mathbb{E}$ is sketched in Fig. 3, which is the space between the two regions in dark color. The two dark-colored regions themselves represent boundaries of intersected neighboring dome-like bodies. Observe marginal PDFs with respect to x_2 for the three locations $r-\delta$, r and $r+\delta$, which are presented by three Gaussian PDF curves on the $x_2 - f(x_1, x_2)$ plane with means $\mu(r-\delta)$, $\mu(r)$ and $\mu(r+\delta)$, respectively. It is worth mentioning that shapes of the three curves are the same, which is determined by the variance of Gaussian

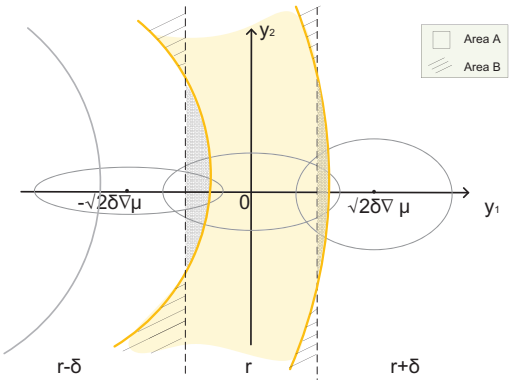

Fig. 4. Graphical illustration of region $\mathbb{E}$

noise. This is because Gaussian noise at different locations in a small neighborhood of the physical space are presenting indistinguishable randomness, which have been acknowledged by extensive studies [13], [14]. Due to symmetry of the dome-like bodies, the same thing happens to the marginal PDFs with respect to x_1.

If the temporal correlation of the RSS is not considered, fingerprints can be observed at different time points with respect to the same AP are independent at each location; therefore, the randomness of the RSS can only be characterized in a 2-D curve of the marginal PDF as shown in Fig. 3. Using such randomness to evaluate the performance limit of fingerprinting localization is the basic idea in [13].

Our work in this paper characterizes randomness of the RSS with the dome-like bodies as shown in Fig. 3, where the temporal correlation of the signal is taken into account. We can see that our model presents a more accurate description of the randomness of the RSS, where a straightforward observation is the increase of a dimension. Such a model of the RSS provides more distinguishable characteristics of a location compared with that in [13], thus provides criteria of finer-granularity for localization. This is the fundamental reason why the accuracy performance bound of localization derived in [13] can be further improved if the RSS temporal correlation is taken into account.

B. Analysis on Region $\mathbb{E}$

Since the location estimation is performed based on fingerprints reported by the user, studying properties of $\mathbb{E}$ can help reveal how the system estimates the user's location. Intuitively, if we project the image in Fig. 3 onto the $y_1 - y_2$ coordinates system, the resulted image should be that as shown in Fig. 4. The region in yellow should be the projection of the space $\mathbb{E}$, and the two curves in yellow should be boundaries of the region. Consequently, if a user's reported fingerprints fall into the area left to $\mathbb{E}$, the user is more likely at the location $r - \delta$; if the reported fingerprints fall into the area right to $\mathbb{E}$, the user is more likely at the location $r + \delta$. We are to reveal that the boundaries of $\mathbb{E}$ are in the shape of hyperbolic curve with interesting properties, and then reveal challenges for accurately describing the region $\mathbb{E}$ with corresponding analysis provisioned.

1) Boundaries of Region $\mathbb{E}$: Substituting Eq. (7) into Eq. (9), we obtain the following inequality:

$$\frac{1}{2\pi\sigma^2\sqrt{\lambda_1\lambda_2}}e^{-\frac{1}{2\sigma^2}(\frac{y_1^2}{\lambda_1}+\frac{y_2^2}{\lambda_2})} \geq \frac{1}{2\pi\sigma^2\sqrt{\lambda_1^{\pm}\lambda_2^{\pm}}}e^{-\frac{1}{2\sigma^2}(\frac{(y_1\pm\sqrt{2}\delta\bigtriangledown\mu)^2}{\lambda_1^{\pm}}+\frac{y_2^2}{\lambda_2^{\pm}})}, \tag{10}$$

where λ_1, λ_2 are scaling factors of ellipse axes for Gaussian PDF at position r, and $\lambda_1^{\pm}, \lambda_2^{\pm}$ are scaling factors at adjacent positions $r \pm \delta$. Specifically,

$$\begin{aligned} \lambda_1 = \frac{\sqrt{2}(1+\rho)}{2}, \lambda_2 = \frac{\sqrt{2}(1-\rho)}{2}; \\ \lambda_1^{\pm} = \frac{\sqrt{2}(1+\rho^{\pm})}{2}, \lambda_2^{\pm} = \frac{\sqrt{2}(1-\rho^{\pm})}{2}. \end{aligned} \tag{11}$$

Symbols $\rho, \rho^{\pm}$ are the autocorrelation coefficients for the Gaussian distribution at r and $r \pm \delta$, respectively. After simplification, they are equivalent to:

$$\begin{cases} (\frac{y_1^2}{\lambda_1}+\frac{y_2^2}{\lambda_2}) - (\frac{(y_1+\sqrt{2}\delta\bigtriangledown\mu)^2}{\lambda_1^{+}}+\frac{y_2^2}{\lambda_2^{+}}) \leq \ln\frac{\lambda_1\lambda_2}{\lambda_1^{+}\lambda_2^{+}}; \\ (\frac{y_1^2}{\lambda_1}+\frac{y_2^2}{\lambda_2}) - (\frac{(y_1-\sqrt{2}\delta\bigtriangledown\mu)^2}{\lambda_1^{-}}+\frac{y_2^2}{\lambda_2^{-}}) \leq \ln\frac{\lambda_1\lambda_2}{\lambda_1^{-}\lambda_2^{-}}, \end{cases} \tag{12}$$

which is the specific expression of $\mathbb{E}$ in the sample space. The boundaries of $\mathbb{E}$ can be obtained when the equality holds.

In order to better understand properties of the boundaries, we transform the expressions in inequalities (12) into a general form

$$Ay_1^2 + By_1y_2 + Cy_2^2 + Dy_1 + Ey_2 + F = 0, \tag{13}$$

where the discriminant Δ equals to

$$\Delta = B^2 - 4AC, \tag{14}$$

and $A = \frac{1}{\lambda_1} - \frac{1}{\lambda_1^{\pm}}$, $C = \frac{1}{\lambda_2} - \frac{1}{\lambda_2^{\pm}}$. Since $B = 0$, $AC < 0$, then $\Delta > 0$. This means that the two boundaries of $\mathbb{E}$ are in the shape of the hyperbolic curve, where the two foci are on axis y_1.

Note that if $A = C$ and $B = 0$, both of the boundaries are straight lines in parallel. $A = C$ and $B = 0$ also mean that $\lambda_1 = \lambda_2$, $\lambda_1^{\pm} = \lambda_2^{\pm}$, which is to say that measurements with respect to the same AP at different time points are totally independent. This is a degenerated scenario without considering temporal correlation as shown in [13]. The resulted straight-line boundaries are the same as corresponding boundaries of $\mathbb{E}$ in [13]. This is actually corroborating our current result about the shape of boundaries.

2) Accurate Description of $\mathbb{E}$: Although we have a basic idea about boundaries of $\mathbb{E}$, it is still non-trivial to theoretically prove that the region $\mathbb{E}$ is the same as the intuition as shown in Fig. 4. Imagine the detailed scenario that two surfaces representing two joint Gaussian PDFs are intersecting with each other. There are actually two curves of intersection, as

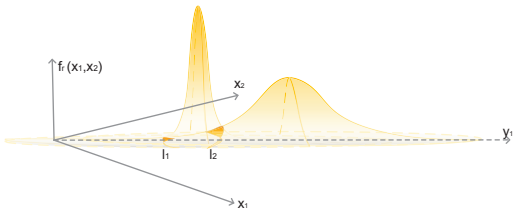

Fig. 5. Intersection of two Gaussian PDFs.

the two curves l_1 and l_2 illustrated in Fig. 5. This can be mathematically proved through simple derivation by constructing an equation between the two joint Gaussian PDFs.

It is slightly tricky to understand Fig. 3 and Fig. 5. Projections of those domes on planes x_1-$f(x_1, x_2)$ and x_2-$f(x_1, x_2)$ are the same in profile, because this is actually ignoring the temporal correlation of the RSS. Mathematically, the covariance matrix of $f_r(x_1, x_2)$ becomes variance σ^2 as the autocorrelation coefficient $\rho = 0$. However, those joint Gaussian PDFs factually have different autocorrelation coefficients denoted by ρ and $\rho^{\pm}$, as shown in Fig. 3; therefore, if we project those domes on the plane y_1-$f(x_1, x_2)$, the resulted image is just that illustrated in Fig. 5.

In the perspective of engineering, the system considers that observing fingerprints around the l_1 is with very low probability if the user is at r, thus it is more meaningful to consider the boundary represented by l_2, in order to ensure an expected localization reliability as high as possible. It is worth mentioning that fingerprints such as those around l_1 indeed can be observed in practice. In this case, the system will estimate the location of the user is at r', where $f_{r'}(y1, y2)$ has a higher value, although the user is factually at r. Such errors can not be avoided in the fingerprinting based approach, since small probability events do happen.

We can see that the opening orientation of the boundaries illustrated in Fig. 3 is to the left. Refer to equalities (11), (12) and Fig. 3, if $\rho^- < \rho < \rho^+$, the physical meaning of the inequalities (12) is that: all points with the distance differences between $r - \delta$ to r and r to $r + \delta$ are less than a constant. The opening orientation is to the left, according to the definition of the hyperbola. If $\rho^- > \rho > \rho^+$, the physical meaning of the inequalities (12) is that: all points with the distance differences between r to $r - \delta$ and $r + \delta$ to r are less than a constant. The opening orientation is to the right. For convenience of presentation, we here abuse the coordinate in the physical space and use the coordinate to represent the corresponding RSS values in the y_1 axis.

This means that the opening orientation of boundaries are actually determined by the degree of temporal correlation of the RSS at different locations. Moreover, no matter the relationship among ρ and $\rho^{\pm}$, the inequalities of (12) show that the area of $\mathbb{E}$ is in the middle of the two boundaries. As a matter of fact, if we specifically consider the real situation under study, it should be the case $\rho^- < \rho < \rho^+$. Recall our 1-D physical model, where the AP is located at the origin of an 1-D coordinate axis and $r - \delta$, r and $r + \delta$ are distance to the AP. The farther the location is from the AP, the stronger the temporal correlation of the observed RSS will be; consequently, the orientations of the two boundaries should be to the left as shown in Fig. 4.

C. Influence of Temporal Correlation on Accuracy of Localization

We can further verify our theory by examining the expected localization result given special fingerprints. The point $(-\sqrt{2}\delta\nabla\mu,\ 0)$ in Fig. 4 is special, which makes $f_{r-\delta}(-\sqrt{2}\delta\nabla\mu, 0)$ to achieve the maximum value. This means that if a user reports fingerprints $(-\sqrt{2}\delta\nabla\mu,\ 0)$, the system definitely should estimate the user's location to be at $r - \delta$. Substituting $(-\sqrt{2}\delta\nabla\mu,\ 0)$ into the first inequality of (12), A natural consequence is supposed to be that the point $(-\sqrt{2}\delta\nabla\mu,\ 0)$ is definitely to the left of the left boundary of $\mathbb{E}$. However, we are surprised to find that it is possible for the point $(-\sqrt{2}\delta\nabla\mu,\ 0)$ to be within the region $\mathbb{E}$. That is, the point $(-\sqrt{2}\delta\nabla\mu,\ 0)$ is to the right of the left boundary of $\mathbb{E}$. This can happen if we set δ to be very small and the difference between ρ^- and ρ to be very large. The grey curve shown in Fig. 4 is the resulted boundary if we choose special values of δ and ρ. This event can lead to errors of location estimation, because a user definitely should be localized at $r - \delta$ is in fact localized at r.

The root cause of the phenomenon is that the choice of δ and ρ in a theoretical perspective may not comply with the real situation. In the real world, the temporal correlation in a small neighborhood with respect to the same AP should be varying smoothly. Consequently, if δ is small, the difference between ρ^- and ρ is supposed to be insignificant.

We now compare localization results yielded by considering and ignoring the temporal correlation of the RSS. Recall the study in [13] ignores the temporal correlation of the RSS. The region $\mathbb{E}$ in this case is the region between the two dashed lines as shown in Fig. 4. Consider shadowed areas B covered with solid lines. If the user's reported fingerprints fall into such areas, it means that the user supposed to be localized at r is mistakenly localized at $r - \delta$, or the user supposed to be localized at $r + \delta$ is mistakenly localized at r. Similarly, consider the grey areas A. If the user's reported fingerprints fall into such areas, it means that the user supposed to be localized at $r - \delta$ is mistakenly localized at r, or the user supposed to be localized at r is mistakenly localized at $r + \delta$. That is, considering temporal correlation can improve the accuracy of location estimation by providing more accurate criteria for making judgement.

Theoretically, the reliability of the localization is the probability that the user's reported fingerprints fall within the region $\mathbb{E}$, so that the user is localized at δ neighborhood of r. Denote the area between the two dashed lines as T. The reliability of the case where temporal correlation is now considered is

$$R(\delta, r, \sigma) = \int_T f(\mathbf{Y}) d(\mathbf{Y}) = \int_{-\frac{1}{2}\delta\nabla\mu}^{\frac{1}{2}\delta\nabla\mu} f(\mathbf{Y}) d(\mathbf{Y}), \quad (15)$$

where $f(\mathbf{Y})$ is the joint Gaussian PDF with respect to fingerprints $\mathbf{Y}$. Consequently, the reliability improvement by the temporal correlation is

$$\Delta R(\delta, r, \sigma, \rho) = \int_{T'-T} f(\mathbf{Y}) d(\mathbf{Y}), \tag{16}$$

where we use T' to denote the area between the two hyperbolas.

V. High-Dimensional Temporal Correlation for Localization

A. High-Dimensional Temporal Correlation

We now extend our analysis to high-dimensional temporal correlation for localization. In this case, the corresponding multivariate Gaussian distribution is with high dimension and covariance matrix $\mathbf{\Sigma}$ is with high rank. Suppose that we consider the temporal correlation of m dimension, then

$$f_{\mathbf{r}}(\mathbf{x}|\mu, \mathbf{\Sigma}) = \frac{1}{(2\pi)^{\frac{m}{2}} |\mathbf{\Sigma}|^{\frac{1}{2}}} e^{-\frac{1}{2}\Delta^2}, \tag{17}$$

where the Mahalanobis distance Δ is now as:

$$\Delta^2 = (\mathbf{x} - \mu)^T \mathbf{\Sigma}^{-1} (\mathbf{x} - \mu). \tag{18}$$

Similar to the analysis procedure for the 2-dimensional temporal correlation, we can always find orthogonal eigenvectors $\mathbf{u_i}$ using Gram Schmidt Orthogonallization (GSO) method such that

$$\mathbf{\Sigma} = \sum_{i=1}^{m} \lambda_i \mathbf{u_i} \mathbf{u_i^T}, \quad \mathbf{\Sigma}^{-1} = \sum_{i=1}^{m} \frac{1}{\lambda_i} \mathbf{u_i} \mathbf{u_i^T}, \tag{19}$$

Let $\mathbf{y} = \mathbf{U}(\mathbf{x} - \mu)$, where $\mathbf{U} = [\mathbf{u_1}, \mathbf{u_2}, \ldots, \mathbf{u_m}]^T$ and $\mathbf{U}\mathbf{U}^T = \mathbf{I}$. Then the coordinate $\mathbf{x}$ can be shifted and rotated to $\mathbf{y}$ with Jocobian Matrix $\mathbf{J}$ and $\mathbf{J} = \mathbf{U}^T$. The multivariate Gaussian distribution in $\mathbf{y}$ coordinate is expressed as:

$$f_r(\mathbf{y}|\mu, \mathbf{\Sigma}) = \frac{1}{(2\pi)^{\frac{m}{2}} (\prod_{i=1}^{m} \lambda_i)^{\frac{1}{2}}} e^{-\frac{1}{2} \sum_{i=1}^{m} \frac{1}{\lambda_i} \mathbf{y_i} \mathbf{y_i^T}}. \tag{20}$$

The probability of $r' \in Q$ or observation $\mathbf{x} \in E$ are the same as equation (9). After simplification, it is equal to

$$\begin{cases} \sum_{i=1}^{m} \frac{y_i^2}{\lambda_i} - [\frac{(y_i + \sqrt{2}\delta \bigtriangledown \mu)^2}{\lambda_i^+} + \sum_{i=2}^{m} \frac{y_i^2}{\lambda_i^+}] \leq \ln \prod_{i=1}^{m} \frac{\lambda_i}{\lambda_i^+}, \\ \sum_{i=1}^{m} \frac{y_i^2}{\lambda_i} - [\frac{(y_i - \sqrt{2}\delta \bigtriangledown \mu)^2}{\lambda_i^-} + \sum_{i=2}^{m} \frac{y_i^2}{\lambda_i^-}] \leq \ln \prod_{i=1}^{m} \frac{\lambda_i}{\lambda_i^-}. \end{cases} \tag{21}$$

We define vectors $\mathbf{h_1}, \mathbf{h_2}, \mathbf{h_3}$ as

$$\begin{cases} \mathbf{h_1} = [\frac{y_1}{\sqrt{\lambda_1}}, \frac{y_2}{\sqrt{\lambda_2}}, \ldots, \frac{y_m}{\sqrt{\lambda_m}}], \\ \mathbf{h_2} = [\frac{y_1 + \sqrt{2}\delta \bigtriangledown \mu}{\sqrt{\lambda_1^+}}, \frac{y_2}{\sqrt{\lambda_2^+}}, \ldots, \frac{y_m}{\sqrt{\lambda_m^+}}], \\ \mathbf{h_3} = [\frac{y_1 - \sqrt{2}\delta \bigtriangledown \mu}{\sqrt{\lambda_1^-}}, \frac{y_2}{\sqrt{\lambda_2^-}}, \ldots, \frac{y_m}{\sqrt{\lambda_m^-}}]. \end{cases} \tag{22}$$

The inequality sets (21) can be put as

$$\begin{cases} ||\mathbf{h_1}||^2 - ||\mathbf{h_2}||^2 \leq \sum_{i=1}^{m} \ln \frac{\lambda_i}{\lambda_i^+}, \\ ||\mathbf{h_1}||^2 - ||\mathbf{h_3}||^2 \leq \sum_{i=1}^{m} \ln \frac{\lambda_i}{\lambda_i^-}. \end{cases} \tag{23}$$

It can be seen that the boundaries of $\mathbb{E}$ in this case is a high-dimensional hyperbola.

B. High-Dimensional Sample Space

Based on Maximum Likelihood Estimation (MLE), suppose the measurements for different n APs are independent and considering the temporal correlation of m dimension. Then the region $\mathbb{E}$ should be:

$$\prod_{i=1}^{n} f_r(\mathbf{y}|\mu, \mathbf{\Sigma}) \geq \prod_{i=1}^{n} f_{r \pm \delta}(\mathbf{y}|\mu, \mathbf{\Sigma}). \tag{24}$$

Denote $y_{i,j}$ as the measurement of ith AP at the mth time points. Similar meaning to $\lambda_{i,j}$. Applying the Eq. (20), we have

$$\sum_{i=1}^{n} \sum_{j=1}^{m} \frac{y_{i,j}^2}{\lambda_{i,j}} - \sum_{i=1}^{n} [\frac{(y_{i,1} \pm \sqrt{2}\delta \bigtriangledown \mu_i)^2}{\lambda_{i,1}^{\pm}} + \sum_{j=2}^{m} \frac{y_{i,j}^2}{\lambda_{i,j}^{\pm}}] \leq \sum_{i=1}^{n} \ln \frac{|\mathbf{\Sigma}_i|}{|\mathbf{\Sigma}_i^{\pm}|}. \tag{25}$$

We here construct new vectors $\mathbf{z}_1, \mathbf{z}_2, \mathbf{z}_3$ with transformation matrix as following:

$$\mathbf{z}_1 = \begin{bmatrix} z_{11} \\ z_{12} \\ \vdots \\ z_{1m} \\ z_{21} \\ \vdots \\ z_{nm} \end{bmatrix} = \begin{bmatrix} \frac{1}{\sqrt{\lambda_{11}}} & 0 & \ldots & 0 & 0 & \ldots & 0 \\ 0 & \frac{1}{\sqrt{\lambda_{12}}} & \ldots & 0 & 0 & \ldots & 0 \\ \vdots & \vdots & \ddots & \vdots & \vdots & \ddots & \vdots \\ 0 & 0 & \ldots & \frac{1}{\sqrt{\lambda_{1m}}} & 0 & \ldots & 0 \\ 0 & 0 & \ldots & 0 & \frac{1}{\sqrt{\lambda_{21}}} & \ldots & 0 \\ \vdots & \vdots & \ddots & \vdots & \vdots & \ddots & \vdots \\ 0 & 0 & \ldots & 0 & 0 & \ldots & \frac{1}{\sqrt{\lambda_{nm}}}, \end{bmatrix} \begin{bmatrix} y_{11} \\ y_{12} \\ \vdots \\ y_{1m} \\ y_{21} \\ \vdots \\ y_{nm} \end{bmatrix} \tag{26}$$

and build up transformation matrix T_2 as

$$\mathbf{T_2} = \begin{bmatrix} \frac{1}{\sqrt{\lambda_{11}^+}} & 0 & \ldots & 0 & 0 & \ldots & 0 & \frac{\delta \bigtriangledown \mu_1}{\sqrt{\lambda_{11}^+}} \\ 0 & \frac{1}{\sqrt{\lambda_{12}^+}} & \ldots & 0 & 0 & \ldots & 0 & 0 \\ \vdots & \vdots & \ddots & \vdots & \vdots & \ddots & \vdots & \vdots \\ 0 & 0 & \ldots & \frac{1}{\sqrt{\lambda_{1m}^+}} & 0 & \ldots & 0 & 0 \\ 0 & 0 & \ldots & 0 & \frac{1}{\sqrt{\lambda_{21}^+}} & \ldots & 0 & \frac{\delta \bigtriangledown \mu_2}{\sqrt{\lambda_{21}^+}} \\ \vdots & \vdots & \ddots & \vdots & \vdots & \ddots & \vdots & \vdots \\ 0 & 0 & \ldots & 0 & 0 & \ldots & \frac{1}{\sqrt{\lambda_{nm}^+}} & 0 \\ 0 & 0 & \ldots & 0 & 0 & \ldots & 0 & 1. \end{bmatrix} \tag{27}$$

Then the second vector $\mathbf{z_2}$ can be expressed as

$$\mathbf{z}_2 = \begin{bmatrix} z_{11} \\ \vdots \\ z_{nm} \\ 1 \end{bmatrix} = \mathbf{T_2} \begin{bmatrix} y_{11} \\ \vdots \\ y_{nm} \\ 1 \end{bmatrix} \tag{28}$$

Similarly, define $\mathbf{z}_3$ to be the position $(\mathbf{r} - \vec{\delta})$ as $\mathbf{z}_2$ to be the position $(r + \vec{\delta})$. Applying the vectors $\mathbf{z}_1, \mathbf{z}_2, \mathbf{z}_3$ to inequality (25), we can get

$$\begin{cases} ||\mathbf{z_1}||^2 - ||\mathbf{z_2}||^2 \leq \sum_{i=1}^{n} \ln \frac{|\Sigma_i|}{|\Sigma_i^+|} \\ ||\mathbf{z_1}||^2 - ||\mathbf{z_3}||^2 \leq \sum_{i=1}^{n} \ln \frac{|\Sigma_i|}{|\Sigma_i^-|} \end{cases} \tag{29}$$

These inequations indicate that the difference of distance to two different points is a constant. By the definition of hyperbola, the boundaries of $\mathbb{E}$ are in the shape of high-dimensional hyperbola with shearing in different dimensions.

C. Two-Dimensional Physical Space

We define a location in this case as a two-dimensional vector $\vec{r}$ as shown in Fig. 1, and the joint Gaussian PDF after correlation rotation is still the multivariate Gaussian function as in Eq. (20). Then the probability of $\vec{r'} \in Q$ or $\mathbf{x} \in \mathbb{E}$ is

$$\mathbb{E} = \{\mathbf{x} | \prod_{i=1}^{n} f_{\vec{r}}(\mathbf{y}|\mu, \mathbf{\Sigma}) \geq \prod_{i=1}^{n} f_{\vec{r}\pm\vec{\delta}}(\mathbf{y}|\mu, \mathbf{\Sigma})\}, \tag{30}$$

where $\vec{\delta}$ is the difference of the user's real location $\vec{r}$ and estimated location $\vec{r'}$, i.e., $\vec{\delta} = \vec{r} - \vec{r'}$. We use θ to denote the angle between $\vec{r}$ and $\vec{r'}$ ranging from 0 to 2π, as shown in Fig. 1.

Substituting the Eq. (20) into Eq. (30), we rewrite the detailed expression of $\mathbb{E}$ as:

$$\sum_{i=1}^{n} \frac{\mathbf{y}}{\lambda} - \sum_{i=1}^{n} \frac{\mathbf{y} + \vec{\delta} \bigtriangledown \mu(\vec{r}) \cos\theta}{\lambda'} \leq \sum_{i=1}^{n} \ln \frac{|\mathbf{\Sigma}_i|}{|\mathbf{\Sigma}_i'|} \tag{31}$$

As the temporal correlation of the RSS is relatively stable in a small neighborhood, we can use $\bigtriangledown\rho(\vec{r})$ to denote its gradient at position $\vec{r}$. Refer to Fig. 1, a circle in the 2-D physical space is formed by rotating $\vec{\delta}$ from 0 to 2π. Consequently, the region $\mathbb{E}$ is formed with hyperbolas in different dimensions, which is as the body shown in the 3-D sample space in Fig. 6. The shape of the intersection between $\mathbb{E}$ and the corresponding orthogonal plane is irregular as shown in Fig. 6, this is because the temporal correlation in different locations can be different, which makes the curvature of the hyperbolas different from each other.

VI. Experimental Results

In this section, we demonstrate experimental results to show the performance difference between the system utilizing and the system ignoring temporal correlation of the RSS. The experiments are conducted in a hallway to verify our analysis for the 1-D physical space. We use two mobile devices to measure the RSSes from one AP at two different locations that is 2 meters from each other. In order to differentiate temporal correlations of the two locations, we add noise of people motion to one of the channels from the AP to mobile devices. We measure the RSS value every 100 millisecond for 1k times at each location. Traditional localization estimation

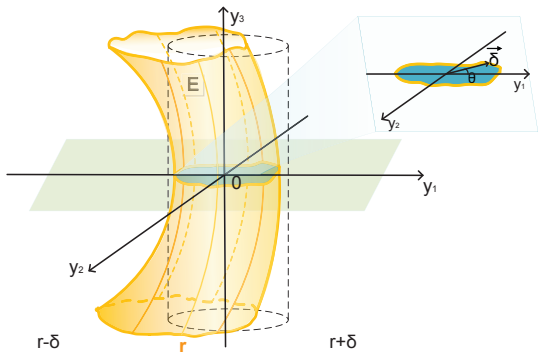

Fig. 6. Region $\mathbb{E}$ in 2-D physical space localization.

processes extract the RSS information independently and build the corresponding PDF in the database, such as the measured RSS distribution shown in Fig. 7, where each curve represents the PDF of each location. The two figures represent two cases, where the first case means that the temporal correlation at each location is distinctive, and the second case means that the two locations' temporal correlations are similar to each other. The regression parameters for the Gaussian PDFs are as shown in Table I.

TABLE I
Fitting 1-D Gaussian parameters

Gaussian	Pic1_r1	Pic1_r2	Pic2_r1	Pic2_r2
amplitude	152.119	391.278	205.92	135.665
mean	-71.574	-59.61	-70.3584	-72.8452
sigma	3.5943	1.409	2.54672	4.10548

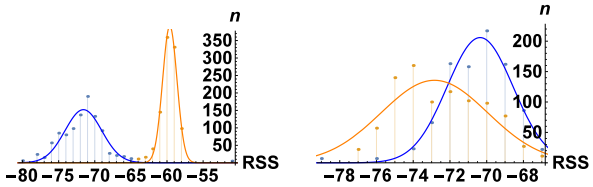

Fig. 7. PDFs of the RSSes

Based on the fingerprints observed above, we now construct the corresponding 2-D temporal correlation PDFs, which are illustrated in Fig. 8(a) and Fig. 8(b). The corresponding regression parameters for the joint 2-D Gaussian PDFs are shown in Table II.

TABLE II
Fitting 1-D Gaussian parameters.

Gaussian	Pic1_r1	Pic1_r2	Pic2_r1	Pic2_r2
A	126.274	254.858	184.975	124.457
μ	-71.5829	-59.5945	-70.3273	-72.8478
σ	2.5122	0.9905	1.7931	2.8962
ρ	0.9877	0.9215	0.977799	0.99263

The experimental results are shown in Fig. 8(c) and Fig. 8 (d), where the blue and yellow dots are fingerprints reported

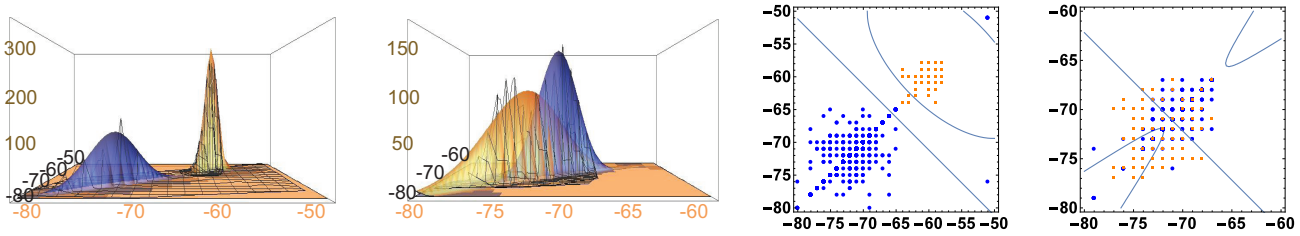

(a) Gaussian Distribution of Exp1

(b) Gaussian Distribution of Exp2

(c) Exp1 Hyperbola Boundary

(d) Exp2 Hyperbola Boundary

Fig. 8. 2-d Gaussian Distribution and Hyperbolic Criteria for Localization

at the first and the second locations, respectively. The curve and straight-line boundaries to separate dots are generated by the system considering and ignoring the temporal correlation, respectively. In both cases shown in Fig. 8(c) and Fig. 8 (d), the curve boundary helps the system make more accurate location estimation. Due to the way of presentation, the seemingly one point on the figures actually represents many fingerprints. The results show that the number of fingerprints whose associated locations have been correctly estimated is much higher with the temporal boundary. We can expect that the performance of the system will be better if more fingerprints are sampled. In order to deal with the small probability event, we put both of arms of the hyperbola in the figure. An interesting finding is that there is a blue dot in the upper right of Fig. 8(c), which can be correctly localized with the temporal boundary.

VII. Conclusions and Future Work

In this paper, we have theoretically shown that the temporal correlation of the RSS can improve accuracy of RSS fingerprinting based indoor localization. In particular, we have constructed a theoretical framework to evaluate how the temporal correlation of the RSS can influence the reliability of location estimation, which is based on a newly proposed radio propagation model considering the time-varying property of signals from a given Wi-Fi AP. Such a theoretical framework was then applied to analyze localization in the one-dimensional physical space, which reveals the fundamental reason why performance improvement of localization can be brought by temporal correlation of the RSS. We have extended our analysis to high-dimensional scenarios and reveal key information for calculating localization reliability. Experiment results corroborate our theoretical analysis. Our future work is to further study the high-dimensional cases.

VIII. Acknowledgement

This work is supported by National Natural Science Foundation of China (No. 61532012, 61572319, U1405251, 61325012, 61271219, 61428205); National Mobile Communications Research Laboratory, Southeast University (No.2012D13, 2014D07); Jiangsu Future Network Research Project No. BY2013095-1-10.

References

[1] Z. Yang, Z. Zhou and Y. Liu, "From RSSI to CSI: Indoor localization via channel response," *ACM Comput. Surv.*, vol. 46, no. 2, pp.1-32, 2013.

[2] H. Liu, Y. Gan, J. Yang, S. Sidhom, Y. Wang, Y. Chen and F. Ye, " Push the Limit of WiFi based Localization for Smartphones," in *Proc. ACM MobiCom*, 2012, pp. 305–316.

[3] H. Liu, J. Yang, S. Sidhom, Y. Wang, Y. Chen and F. Ye, " Accurate WiFi Based Localization for Smartphones Using Peer Assistance," *IEEE Transactions on Mobile Computing* , vol. 13, no. 10, pp.2199–2214, Oct. 2013.

[4] A. Rai, K. K. Chintalapudi, V. N. Padmanabhan and R. Sen, "Zee: zero-effort crowdsourcing for indoor localization," in *Proc. ACM MobiCom*, 2012, pp. 293–304.

[5] S. Fang, B. Lu and Y. Hsu, "Learning location from sequential signal strength based on GSM experimental data," *IEEE Transactions on Vehicular Technology*, vol. 61, no. 2, pp.726–736, Feb. 2012.

[6] S. Fang and T. Lin, "A dynamic system approach for radio location fingerprinting in wireless local area networks." *IEEE Transactions on Communications*, vol. 58, no. 4, pp.1020–1025, April 2010.

[7] S. Kuo and Y. Tseng, "A scrambling method for fingerprint positioning based on temporal diversity and spatial dependency." *IEEE Transactions on Knowledge and Data Engineering*, vol. 20, no. 5, pp.678-684, May 2008.

[8] G. Chandrasekaran, M. A. Ergin, J. Yang, S Liu, Y. Chen, M. Gruteser and R. P. Martin, " Empirical evaluation of the limits on localization using signal strength," in *Proc. IEEE SECON*, 2009, pp. 1–9.

[9] N. Patwari, J. Ash, S. Kyperountas, I. Hero, A.O., R. Moses and N. Correal, "Locating the nodes: cooperative localization in wireless sensor networks, *IEEE Signal Processing Magazin*, vol. 22, no. 4, pp.55–69, 2005.

[10] N. Patwari, A. O. H. III, M. Perkins, N. S. Correal and R. J. ODea, Relative location estimation in wireless sensor networks, *IEEE Transactions on Signal Processing*, vol. 51, no. 8, pp.2137–2148, 2003.

[11] M. Angjelichinoski, D. Denkovski, V. Atanasovski and L. Gavrilovska, " Cramér-Rao Lower Bounds of RSS-Based Localization With Anchor Position Uncertainty *IEEE Transactions on Information Theory*, vol. 61, no. 5, pp. 2807-2834, May 2015.

[12] K. Chintalapudi, A. Padmanabha Iyer and V. N. Padmanabhan, "Indoor localization without the pain," in *Proc. ACM MobiCom*, 2010, pp. 173–184.

[13] Y. Wen, X. Tian, X. Wang and S. Lu, "Fundamental limits of RSS fingerprinting based indoor localization," in *Proc. IEEE INFOCOM*, 2015.

[14] K. Kaemarungsi and P. Krishnamurthy, "Properties of indoor received signal strength for WLAN location fingerprinting, in *Mobile and Ubiquitous Systems: Networking and Services, IEEE* , August 2004, pp. 14–23.

[15] K. Kaemarungsi and P. Krishnamurthy, "Modeling of indoor positioning systems based on location fingerprinting," in *IEEE INFOCOM*, March 2004, pp. 1012-1022.

[16] E. Elnahrawy, X. Li and R. P. Martin, "The limits of localization using signal strength: A comparative study," in *Proc. IEEE SECON*, 2004, pp. 406–414.

[17] K. Chintalapudi, A. Padmanabha Iyer and V. N. Padmanabhan, "Indoor localization without the pain," in *Proc. ACM MobiCom*, 2010, pp. 173–184.